Expression of WNT5A in Idiopathic Pulmonary Fibrosis and Its Control by TGF-β and WNT7B in Human Lung Fibroblasts

Donna R. Newman, W. Shane Sills, Katherine Hanrahan, Amanda Ziegler, Kathleen McGinnis Tidd, Elizabeth Cook, and Philip L. Sannes

Department of Molecular Biomedical Sciences, Center for Comparative Medicine and Translational Research, College of Veterinary Medicine, and Center for Human Health and the Environment, College of Sciences, North Carolina State University, Raleigh, North Carolina (DRN, WSS, KH, AZ, KMT, EC, PLS)

Summary

The wingless (Wnt) family of signaling ligands contributes significantly to lung development and is highly expressed in patients with usual interstitial pneumonia (UIP). We sought to define the cellular distribution of Wnt5A in the lung tissue of patients with idiopathic pulmonary fibrosis (IPF) and the signaling ligands that control its expression in human lung fibroblasts and IPF myofibroblasts. Tissue sections from 40 patients diagnosed with IPF or UIP were probed for the immunolocalization of Wnt5A. Further, isolated lung fibroblasts from normal or IPF human lungs, adenovirally transduced for the overexpression or silencing of Wnt7B or treated with TGF-β1 or its inhibitor, were analyzed for Wnt5A protein expression. Wnt5A was expressed in IPF lungs by airway and alveolar epithelium, smooth muscle cells, endothelium, and myofibroblasts of fibroblastic foci and throughout the interstitium. Forced overexpression of Wnt7B with or without TGF-β1 treatment significantly increased Wnt5A protein expression in normal human smooth muscle cells and fibroblasts but not in IPF myofibroblasts where Wnt5A was already highly expressed. The results demonstrate a wide distribution of Wnt5A expression in cells of the IPF lung and reveal that it is significantly increased by Wnt7B and TGF-β1, which, in combination, could represent key signaling pathways that modulate the pathogenesis of IPF. (J Histochem Cytochem 64:99–111, 2016)

Keywords

Introduction

Idiopathic pulmonary fibrosis (IPF), or usual interstitial pneumonia (UIP), is a disease characterized by the failure of alveolar epithelial surfaces to repair effectively following damage of unknown origin. This results in epithelial hyperplasia, hypertrophy, and metaplasia, the expansion of a heterogeneous population of long-lived myofibroblast-like cells, and an expanded fibrous extracellular matrix (ECM) with advancing loss of normal pulmonary architecture and function (Schwartz et al. 1994; Green 2002). One of the key features of this disorganized restructuring are fibroblastic foci (FF), indicative of progressive disease, which have been shown to comprise a complex, interconnected reticulum extending from the pleural surface into the core of the lung parenchyma (Cool et al. 2006). FF are typically sub-epithelial and can be found near normal pulmonary tissue (Katzenstein and Myers 1998; Katzenstein et al. 2002).

Corresponding Author:
Philip L. Sannes, Department of Molecular Biomedical Sciences, College of Veterinary Medicine, North Carolina State University, 1051 William Moore Drive, Raleigh, NC 27607 USA.
Email: plsannes@ncsu.edu

Their development leads to end-stage fibrosis with shrinking functional pulmonary structure (Kapanci et al. 1995; Katzenstein and Myers 1998; Katzenstein et al. 2002).

A variety of factors have been demonstrated to be involved or otherwise drive the cellular and reorganized ECM features common to IPF. TGF-β is probably best known for its regulatory influences on fibrogenesis in IPF (Chilosi et al. 2003; Fernandez and Eickelberg 2012) by fostering the growth of myofibroblasts and the expansion of fibrillar collagen and various components of the ECM, which, in many cases, is cooperatively controlled by Wnt signaling (Broekelmann et al. 1991; Scotton and Chambers 2007; Salazar, Lankford, and Brody 2009). Wnt7B gene expression has been reported to be upregulated in IPF lungs (Konigshoff et al. 2008) and found to be localized in tissue sections within distinct sites that include cells and the ECM within FF of IPF lungs (Meuten et al. 2012). Wnt7B is known to be important during early lung development as a signaling glycopeptide that directs proliferation of adjacent epithelium and mesenchymal cells (Rajagopal et al. 2008) and controls the growth of vasculature (Shu et al. 2002). This has led to the suggestion that Wnt7B may be reactivated to significantly impact the progression of IPF in the adult lung (Morrisey 2003; Meuten et al. 2012).

Wnt5A has been shown to be involved in distal lung morphogenesis (Li et al. 2002), in part through the regulation of sonic hedgehog (SHH) and fibroblast growth factor 10 (FGF10) (Li et al. 2005). It has also been demonstrated to be involved in alveolarization (Boucherat et al. 2007) and airway and vascular tubulogenesis (Loscertales et al. 2008), and in the regulation of pulmonary vascular development (Cornett et al. 2013). Wnt5A has also been shown to be significantly upregulated in UIP/IPF and to promote proliferation and prevent apoptosis in fibroblasts from patients with UIP/IPF (Vuga et al. 2009). Its fibrogenic qualities are also demonstrated by its up-regulation in sarcoidosis (Levänen et al. 2011), ventilator-induced pulmonary fibrosis (Villar, et al. 2011), and liver fibrosis (Rashid et al. 2012). Recent studies have demonstrated an increased expression of Wnt5A in smooth muscle cells in asthma and its necessity for TGF-β-induced production of ECM (Kumawat et al. 2013). We show here that Wnt5A is widely distributed in and expressed by epithelium, fibroblasts, and smooth muscle cells of IPF lungs and is regulated by TGF-β1 and Wnt7B.

Materials & Methods

Immunostaining

Tissue blocks of 60 formalin-fixed lung tissue samples were obtained from the Lung Tissue Research Consortium (LTRC). The samples used for immunostaining came from patients who had previously been placed into one of three groups: (1) patients with forced vital capacities (FVCs) >80% (normal, or no specified major or minor diagnosis, *n*=3); (2) patients with FVCs between 50% to 80% [major final clinical diagnosis as interstitial lung disease (ILD, *n*=8) and minor final clinical diagnosis as usual interstitial pneumonia/idiopathic pulmonary fibrosis (UIP/IPF)]; and (3) patients with FVCs <50% (major final clinical diagnosis of ILD and minor final clinical diagnosis as UIP/IPF, *n*=8). No other patient identifiers were provided, and their anonymity and confidentiality were preserved. The study was approved by the North Carolina State University Institutional Review Board. Paraffin blocks were sectioned and stained with hematoxylin and eosin (H&E) and examined by a board-certified pathologist to independently confirm/reclassify initial clinical diagnoses (Meuten et al. 2012).

Sections randomly selected from each of the three groups (10 from each, 30 total) were treated with citrate buffer for antigen retrieval and probed with a rabbit polyclonal anti-human Wnt5A antibody that was raised against a synthetic peptide between aa180-229 of NP_003383 and immunoaffinity purified (LS-B4565, lot UZ03; LifeSpan Biosciences, Inc., Minneapolis, MN) and used at a dilution of 5 µg/ml overnight at 4°C. A rabbit monoclonal anti-human Wnt5A/B antibody (#2530, lot 2; Cell Signaling Technology, Danvers, MA) for western blot served as a negative control, as it was not certified for immunohistochemistry (IHC). A mouse monoclonal anti-α-smooth muscle actin (α-SMA) antibody (A5228, lot 110M4795; Sigma-Aldrich, St. Louis, MO) was used at a 1:500 dilution for 2 hr at room temperature. A rabbit polyclonal anti-human SP-C antibody raised against the full-length protein (sc-13979; Santa Cruz Biotechnology, Inc., Dallas, TX) was used at a 1:100 dilution for 2 hr at room temperature. All primary incubations were followed by peroxidase-labeled secondary antibodies (Dako LSAB+ [Dako Laboratories; Carpinteria, CA] or ImmPRESS Polymer Detection Reagent [Vector Laboratories; Burlingame, CA]) and visualized with Nova Red (Vector Laboratories). Control samples substituted normal rabbit serum or ascites fluid for the primary antibody at an equivalent protein concentration. To demonstrate specificity of the Wnt5A stain, Wnt5A antibody (LifeSpan) was incubated overnight at 4°C with its immunizing peptide P41221 (LS-E11228, LifeSpan) at a 20-fold molar excess before its use in IHC. Sections were counterstained with methylene blue or Celestine blue and routinely mounted. When appropriate, adjacent or parallel sections were used to compare the localization of different target molecules in the same site.

Cell Preparations

Human alveolar type II (hAT2) cells and lung fibroblasts (hLF) were isolated by elastase digestion from organ donor lungs provided by the Tissue Procurement and Cell Culture Core of the Cystic Fibrosis/Pulmonary Research and

Treatment Center (the Core) at the University of North Carolina at Chapel Hill (UNC-CH). Organ donor lungs not suitable for transplantation but still useful for cell harvest were obtained by the Core through the National Disease Research Interchange (Philadelphia, PA). All human materials were handled per protocols approved by the UNC Institutional Committee on the Protection of the Rights of Human Subjects (IRB) and strict procedures were followed to ensure patient confidentiality. Age, sex, and ethnic background were not considered when obtaining specimens and are expected to reflect those of the U.S. population of general organ donors. Uniform consent is not practicable or feasible because donors were deceased (i.e., cadaveric organ donors). For these specimens, consent for research use of tissue was obtained from an authorized representative of the deceased by the organ procurement agency and has been deemed acceptable by the UNC IRB. The waiver does not adversely affect the rights and welfare of the tissue donors because of procedures to insure subject anonymity. The use of anonymous cadaveric organ donor tissue is considered to be exempt from IRB review. Following isolation (see below), hAT2 cells were maintained in low-glucose DMEM medium (Life Technologies; Grand Island, NY) supplemented with 10% FBS and gentamicin (both from Life Technologies) and antibiotic-antimycotic solution (Cellgro; Manassas, VA). Fibroblasts were maintained in high-glucose DMEM (Cellgro) with the same supplements.

Fibroblasts were also isolated from tissue obtained from patients with known IPF undergoing lung transplant, recruited from the Interstitial Lung Disease Clinic of Duke University Hospitals before their day of transplant. Their evaluation was performed as part of clinical care within this specialty clinic and includes pulmonary function tests, chest CT, serological evaluation, and possible biopsy. All subjects provided written informed consent to participate and to donate a sample of their lung tissue following transplant. All patient medical information was de-identified such that all tissue obtained for fibroblast isolation was completely anonymous to this investigation other than a diagnosis of IPF.

Cell Isolation and Culture

Primary hAT2 cells were isolated according to a scaled-up, modified version of the Dobbs procedure (Dobbs et al. 1986; Apparao et al. 2010) and fibroblast-depleted using an anti-Thy-1 antibody (AS02; EMD Chemicals, Gibbstown, NJ) and pan-mouse IgG Dynabeads (Invitrogen; Carlsbad, CA), as previously described (Zhang et al. 2012). Highly pure hAT2 were seeded in low-glucose DMEM/10% FBS on rat-tail collagen-coated tissue culture dishes or cryopreserved. After a medium change the next day, cells were treated and cultured for up to 5 days. Normal human lung fibroblasts (hLFs) were grown out from non-fibroblast-depleted lung cell isolates, purified by two sequential passages, and cryopreserved.

Primary IPF fibroblasts (IPFF) were cultured from IPF donor tissue, which was minced into 1- to 3-mm cubes and plated in flasks with complete high-glucose medium. When they migrated out from the tissue edges, IPFFs were trypsinized and cultured for two sequential passages, then cryopreserved for further experiments.

Human airway smooth muscle cells (hASMCs) were the generous gift of Dr. Julian Solway, University of Chicago. Cells were cultured in high-glucose DMEM:F-12 medium (50/50) (Cellgro) supplemented with 10% FBS, antibiotics, and selected growth factors.

An adherent human kidney epithelial cell line, 293A, was obtained from Life Technologies as a component of its ViraPower Adenoviral Expression kit and cultured in high-glucose DMEM medium with 10% FBS, MEM non-essential amino acids (Life Technologies), and antibiotics.

Plasmid Constructs and Adenovirus Generation

The ViraPower Adenoviral Expression System (Life Technologies) was used to construct an adenoviral vector for the overexpression of human Wnt7B. The Gateway entry clone IOH23284 (Life Technologies) encoding human Wnt7B ending with a stop sequence was combined with pAd-CMV/V5-DEST in a Clonase II LR reaction to generate the adenoviral plasmid pAd-CMV-Wnt7B. A clone with perfect sequence was amplified, cut with PacI, and transfected into 293A cells to generate the CMV-Wnt7B adenovirus. CMV-LacZ adenovirus was generated by linearizing and transfecting into 293A cells the positive expression control plasmid pAd/CMV/V5-GW/lacZ supplied in the pAd/CMV/V5-DEST Gateway Vector kit (V493-20; Life Technologies). Purchased control adenoviruses for overexpression, Ad5.GFP (ADV-GPF-S, lot 02171; QBIOgene, Inc., Montreal, CA), and for silencing, Ad-U6-shRNA(scramble)-GFP (SignaGen Laboratories, Rockville, MD) were amplified in 293A cells to produce CMV-GFP and shScramble adenoviruses, respectively.

Entry plasmids targeting the human Wnt7B gene (NM_058238) for silencing were constructed in the Block-iT U6 entry vector (Life Technologies) according to the manufacturer's instructions, targeting sequences starting at nucleotides 907, 1055, and 1339. A successful clone of each entry construct was flipped into the promoterless adenoviral vector pAd/Block-iT-DEST using Clonase II LR. Plasmids of the correct sequences were amplified, cut with PacI, and transfected into 293A cells to generate shWnt7B adenoviruses. A mixture of all three shWnt7B adenoviruses was effective in silencing Wnt7B in rat lung epithelial cells transduced with CMV-Wnt7B adenovirus for hWnt7B overexpression.

The overexpression plasmid for "Active" Wnt5A-V5 (a gift from Xi He, Addgene plasmid #43813) (MacDonald et al. 2014) was transfected into 293A cells to generate V5-tagged hWnt5A-positive control lysates for western analysis.

Adenoviral Transduction for Overexpression and Silencing, and Cell Treatments

Both Wnt7B and TGF-β1 are present in or near fibroblastic foci (Khalil et al., 1991; Meuten et al., 2012) and could be expected to modulate Wnt5A expression. To model in vivo conditions and potentially enhance Wnt5A expression, some hLF, IPFF, and hASMC cells were transduced (in suspension for 1 hr with occasional re-suspension before plating) with CMV-GFP or CMV-LacZ (control) or CMV-Wnt7B (for Wnt7B overexpression) adenoviruses at 50 MOI (Multiplicity of Infection) for 24–30 hr before overnight quiescence in 0.1% FBS medium and treatment with vehicle (4 mM HCl/1 mg/ml BSA) or recombinant human TGF-β1 (240-B; R&D Systems, Minneapolis, MN) at 5–10 ng/ml for 24–36 hr before termination. HAT2 cells were seeded, allowed to attach overnight, adenovirally transduced with the same overexpression constructs at 20 MOI for 30 hr before quiescence, treated with vehicle or TGF-β1 (10 ng/ml), and harvested on day 5.

In other experiments, Wnt7B was first silenced in hLF and IPFF cells using a mixture of all three shWnt7B adenoviruses or a control silencing hairpin adenovirus (shScramble), at high (200) MOI. Fibroblasts express CAR (Coxsackie-adenovirus receptor) at a low level, but silencing in hLFs and IPFFs was achieved when these cells were transduced at 200 MOI for 1 hr in suspension before plating. Silenced cells (48 hr) were then trypsinized, transduced for GFP or Wnt7B overexpression, plated, and cultured for 24 hr before treatment with DMSO or the TGF-β1 receptor kinase inhibitor SB431542 (Sigma-Aldrich) (10 μM) to inhibit TGF-β1 signaling.

Gene Expression Analysis

Parallel cultures to those for protein expression (below) were processed for total RNA isolation using the RNeasy Plus Mini kit (Qiagen; Valencia, CA). Briefly, cells were drained of medium and lysed in RLT Plus containing β-mercaptoethanol, mechanically disrupted (Shredder columns), depleted of genomic DNA (gDNA Eliminator columns), and processed according to the manufacturer's instructions. Pure RNA (2 μg) was reverse-transcribed using the Applied Biosystems High Capacity cDNA Reverse Transcription kit (Applied Biosystems; Foster City, CA) and diluted to 10 ng/μl cDNA. For gene expression analysis, 100 ng cDNA was combined with TaqMan Gene Expression Master Mix and TaqMan primers and probes (Applied Biosystems) specific for Wnt5A (Hs00998537_m1) or GAPDH (Hs99999905_m1), in duplicate, and subjected to 40 rounds of amplification in a MyiQ iCycler (Bio-Rad Laboratories, Inc., Hercules, CA). Normalized levels of Wnt5A gene expression ($^{\Delta\Delta}Ct$) were graphed in Microsoft Excel (Microsoft Corp., Redmond, WA).

Protein Expression Analysis

Cell cultures were terminated by draining, rinsing once with PBS, and lysing in RIPA Buffer (bioWORLD; Dublin, OH) containing additional protease and phosphatase inhibitors (Roche, Indianapolis, IN) at 1.3× concentration. Lysates were subjected to three rounds of sonication at 5–8 sec each, incubated for 30 min at 4°C with end-over-end rolling, and centrifuged for 15 min at 12,000 rpm, 4°C. Cleared supernatants were quantitated using the Pierce 660 reagent (Thermo Scientific, Rockford, IL) and equal amounts of protein were combined with 4× Laemmli dye + β-mercaptoethanol to achieve a 1× dye concentration.

For western blotting, equal (10 to 15 μg) amounts of protein in Laemmli sample dye were heated to 95°C for 10 min and subjected to electrophoretic separation in MOPS running buffer under reducing conditions at 200 V for 60 min on NuPAGE 4% to 12% Bis-Tris gels (Life Technologies). Proteins were transferred to 0.2-μm nitrocellulose membranes (Bio-Rad) and blocked with Tris-buffered saline containing 0.1% Tween-20 (TBST) and 5% milk for 1 hr. Blocked membranes were incubated with primary antibodies in TBST/5% BSA (TBST/BSA) overnight at 4°C. Primary antibodies used for western blotting included goat anti-human Wnt7B (AF3460, R&D Systems) at 1:1000, rabbit monoclonal anti-human Wnt5A/B (#2530, Cell Signaling Technology) at 1:1000, mouse anti-α-smooth muscle actin (A5228, Sigma-Aldrich) at 1:6000, mouse anti-Vimentin (sc-6260, Santa Cruz Biotechnology) at 1:1500, and mouse anti-human plasminogen activator-1 (PAI-1) (612024; BD Biosciences, San Jose, CA) at 1:5000. Mouse anti-GAPDH (sc-32233), anti-Tubulin mouse monoclonal IgM (sc-8035), and rabbit anti-Vinculin (sc-5573), all from Santa Cruz Biotechnology, were used as loading controls. After washing in TBST, blots were incubated in TBST/5% milk containing secondary antibodies conjugated to horseradish peroxidase (Cell Signaling Technology or Santa Cruz) for 2 hr with agitation. Bands on the membrane were detected by chemiluminescence using SuperSignal West Pico or Dura substrate (Pierce Biotechnology; Rockford, IL) and visualized by autoradiography.

Statistics

Where the dynamics of expression are difficult to see, bands from three separate blots were scanned and quantitative image analysis was done using ImageJ software (NIH;
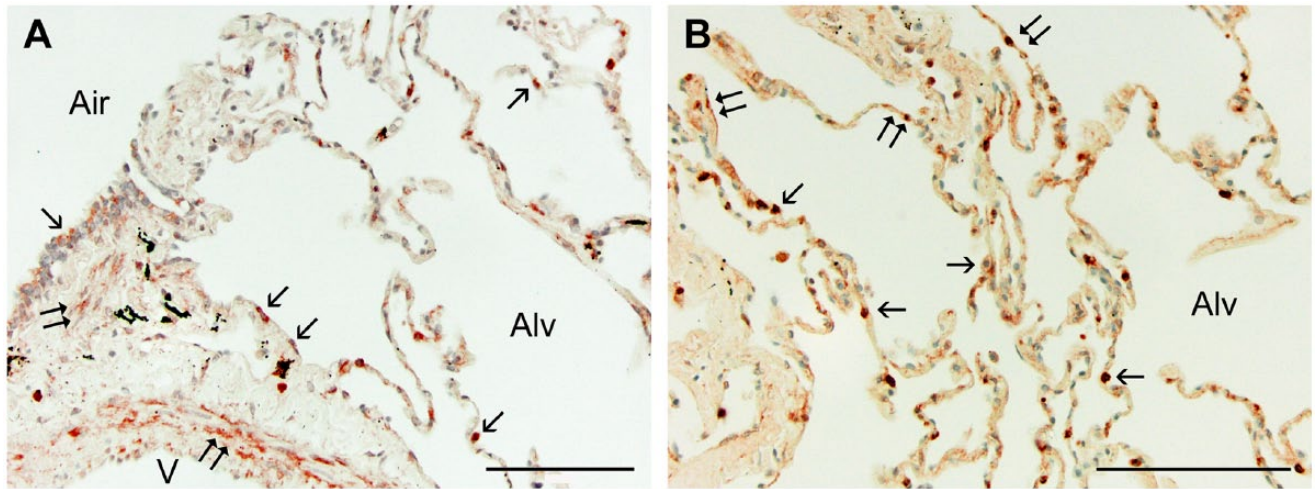
Figure 1. Sections randomly selected from each of the three groups (10 from each, 30 total) were immunostained for Wnt5A, SP-C, or α-SMA, with appropriate controls, as described. (A) Normal human lung tissue treated for the localization of Wnt5A by immunohistochemistry showed reactivity in the smooth muscle (double arrows) of airways (Air) and vessels (V), and in the epithelium (single arrows) of airways (Air) and alveoli (Alv). (B) Higher magnification of lung parenchyma shows reactivity in some but not all cuboidal (alveolar type II; single arrows) and more squamous (alveolar type I; double arrows) cells. All sections were counterstained with methylene blue. Scale, 100 μm.

Bethesda, MD). Experimental groups were compared to "NA" or "CMV-GFP" or "CMV-LacZ" samples for statistical significance by unpaired, two-tailed *t*-test using the Microsoft Excel Analysis ToolPak Add-in software suite, and Excel-generated charts are shown with relevant significances at $p \leq 0.05$ (*) and $p < 0.01$ (**).

Results

In normal human lung, Wnt5A was observed in airway and alveolar epithelial cells, smooth muscle cells, interstitial fibroblasts, and some endothelial cells by immunohistochemistry (Fig. 1A, 1B). In IPF patients, Wnt5A reactivity was more widely observed and strongly expressed in airway and alveolar epithelium, endothelial cells, smooth muscle of airways and vessels of all sizes, and almost all interstitial fibroblasts (Figs. 2A, 3A, 3B). Parallel sections treated with pre-immune rabbit serum (Fig. 2B), a Wnt5A/B antibody not certified for IHC by the manufacturer (Fig. 2C), and a Wnt5A antibody blocked by pre-incubation with its immunizing peptide (Fig. 2D) were non-reactive and lacked label contrast. Airway epithelial cells were reactive for Wnt5A in IPF lungs (Fig. 3A) but not to the extent of alveolar epithelium (Fig. 3A, 3B). The AT2 phenotype of the latter was confirmed by their SP-C reactivity (Fig. 3C). These cells were often hyperplastic, hypertrophic and detached, and sometimes appeared in alveolar and even small airway spaces. The vast majority of fibroblasts in IPF lungs were immunoreactive for Wnt5A, whether located within FF (Figs. 2A, 3B) or simply within the thickened and distorted interstitium characteristic of IPF (Figs. 3A, 3B). Their myofibroblastic phenotype was confirmed by staining positive for α-SMA (Fig. 3D). Of interest was the strong Wnt5A reactivity of all smooth muscle found in IPF lungs, especially that associated with airways (Fig. 3A), and in endothelium of large vessels and in the large number of small vascular elements either trapped in the expanding fibrotic ECM or as neovascular growth common in fibrogenesis (Figs. 2A, 3A, 3B). These cells were also predictably α-SMA-positive (Fig. 3D).

Western blots showed detectable Wnt5A in isolated normal hLFs, which increased with TGF-β1 (5 ng/ml) treatment or after adenoviral transduction for Wnt7B overexpression (Fig. 4). The combination of TGF-β1 and Wnt7B transduction appeared to increase Wnt5A additively (Fig. 4). Similarly, in hASMC cells, Wnt5A was increased by CMV-Wnt7B or TGF-β1 individually, and additively in combination (Fig. 5). Expression of Wnt5A by primary hAT2 cells at day 5 in culture (Fig. 6) was significantly up-regulated by TGF-β1 in control LacZ-overexpressing cells. In hAT2 cells, successful CMV-Wnt7B transduction did not significantly affect Wnt5A or add to the stimulatory effects of TGF-β1 treatment (Fig. 6). Isolated IPFF cells expressed a predictably higher baseline of Wnt5A as compared with hLFs, and it was slightly increased ($p < 0.05$) over controls by CMV-Wnt7B transduction (Fig. 7). Significant TGF-β1-stimulated up-regulation of Wnt5A in control IPFF cells ($p < 0.01$) was apparent after quantitation of scanned western blot bands but was not additive in the Wnt7B-overexpressing cells (Fig. 7).
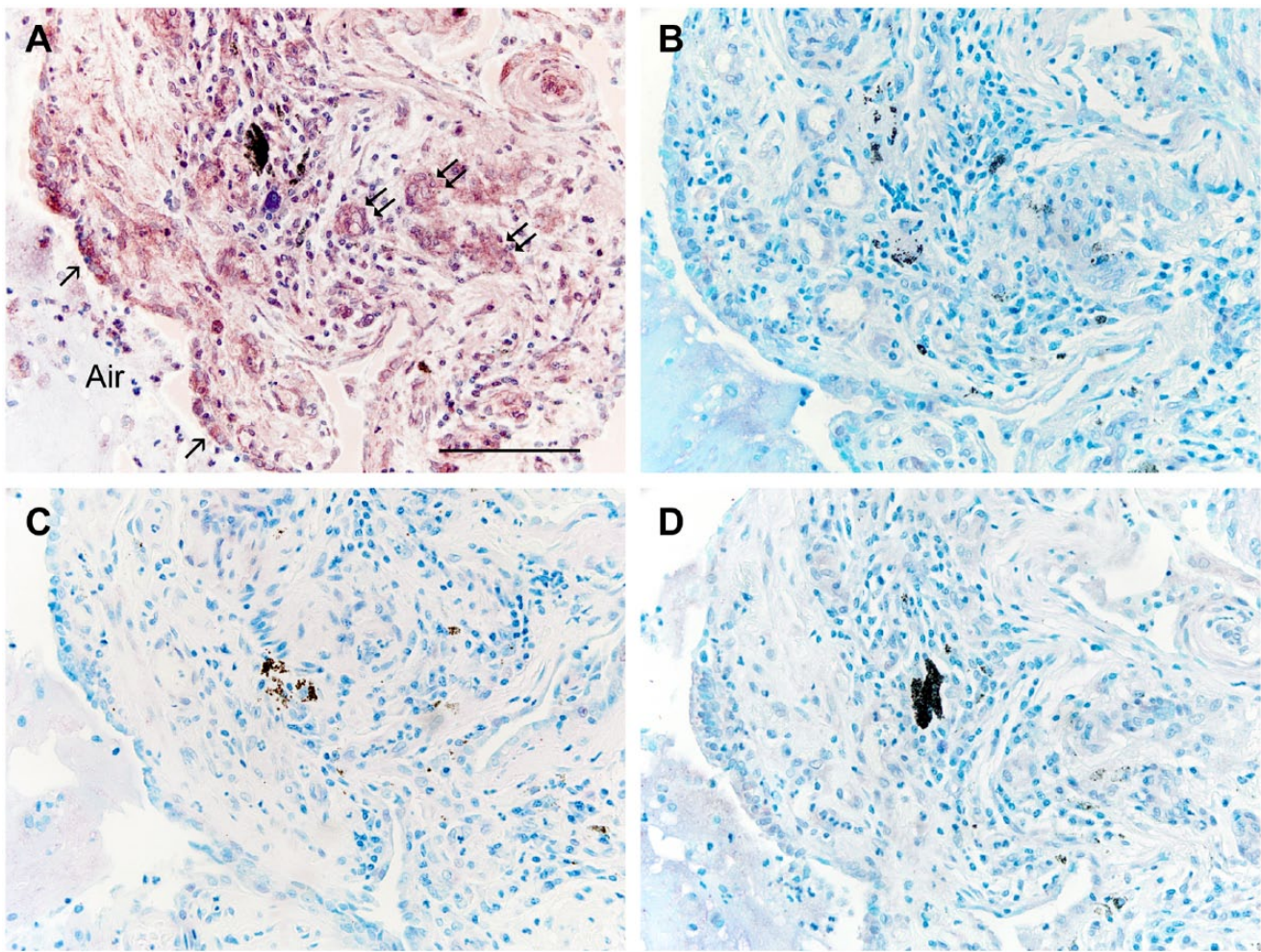
Figure 2. (A) Section from an IPF lung stained for the localization of Wnt5A as in Figure 1. The epithelium lining an airway (Air) expresses Wnt5A (single arrows) as do endothelial cells of small nearby vessels (double arrows). (B–D) Sections adjacent to (A) were treated identically except for: (B) substitution of primary antibody with pre-immune rabbit serum; (C) substitution of the primary antibody with a Wnt5A antibody not certified for IHC-P; or (D) pre-incubation of the primary antibody with its blocking peptide. All antibodies were used at protein concentrations comparable to the primary antibody in (A). All sections were counterstained with methylene blue. Scale, 100 μm.

Control of endogenous and stimulated expression of Wnt5A protein was explored further in hLFs and IPFFs, using Wnt7B-silencing and overexpressing adenoviruses and an inhibitor of TGF-β1 signaling. Both types of fibroblasts were adenovirally transduced (200 MOI) to silence Wnt7B (shWnt7B) or with silencing Control (shScramble) for 48 hr before adenoviral transduction (50 MOI) to overexpress Wnt7B (CMV-Wnt7B) or with overexpression Control (CMV-GFP). After 24 hr, quiescent cells in 0.1% FBS medium were treated with DMSO or 10 μM SB431542 (TGF-β1 Receptor kinase inhibitor) and cultured for an additional 24 hr.

Successful adenovirally transduced overexpression and silencing of Wnt7B in hLFs were confirmed by western blot (Fig. 8A). Adenoviral transduction for forced expression of Wnt7B greatly increased Wnt5A levels over that of the control. Silencing with shWnt7B adenoviruses appeared to increase the expression of Wnt5A over control silencing in both overexpression backgrounds. The loading control, Vinculin, however, was reduced in the shScramble lanes. When the CMV-Wnt7B samples were normalized to the loading control, the apparent increase in Wnt5A by shWnt7B silencing disappeared. SB431542 significantly reduced Wnt7B-stimulated Wnt5A in both silencing backgrounds (Fig. 8B). A downstream target of Wnt7B and TGF-β signaling, α-SMA, was significantly increased by Wnt7B overexpression and decreased in these cells by shWnt7B; however, SB431542 had no effect (Fig. 8A). Overexpression of Wnt7B had little effect on PAI-1, an inhibitor of fibrin breakdown and a marker of matrix
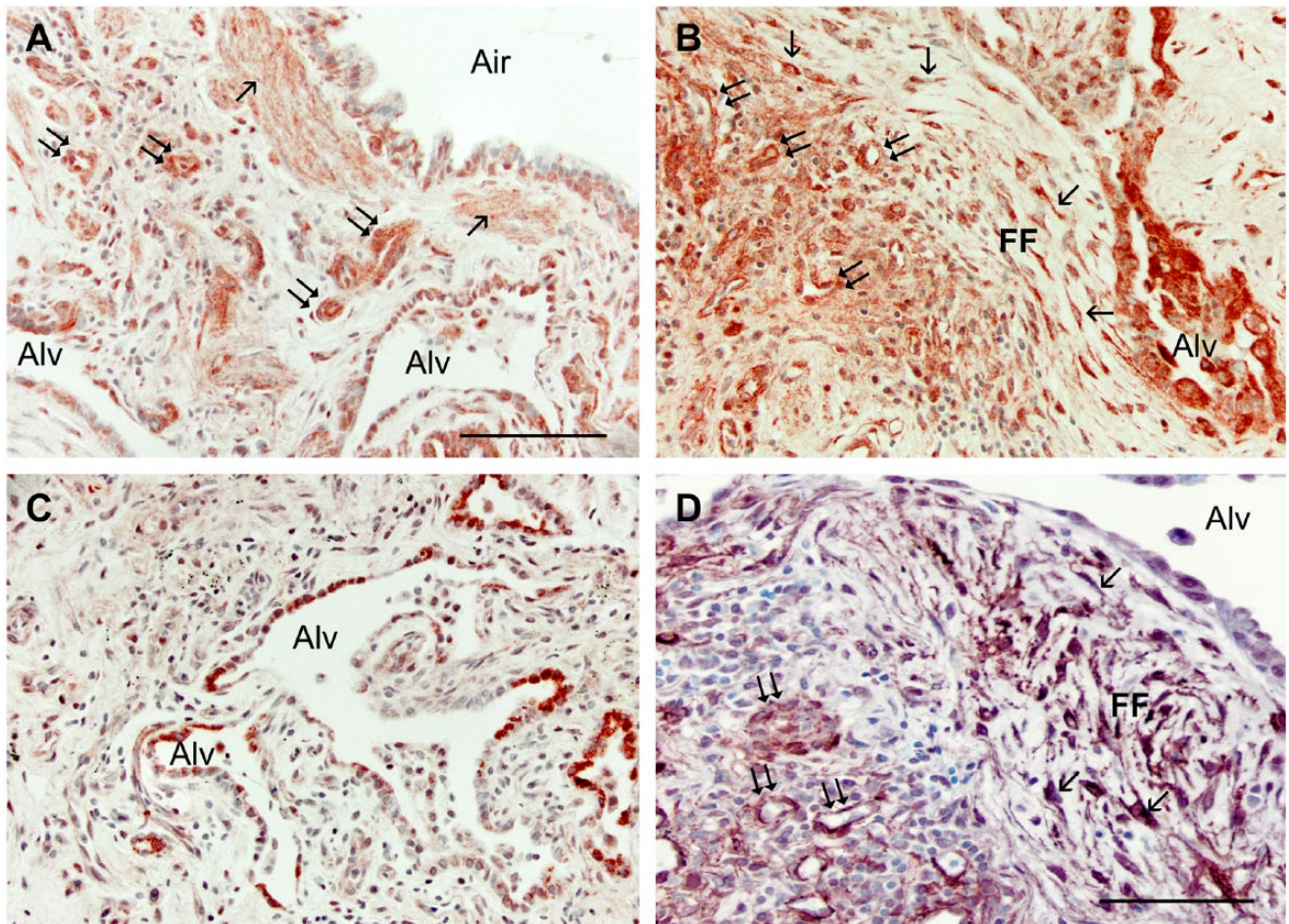
Figure 3. (A) Wnt5A immunostaining of IFP lungs is observed in smooth muscle bundles (single arrows), in the epithelium surrounding an airway (Air), in small vessels (double arrows), and in the epithelium lining the alveoli (Alv). (B) Wnt5A also localizes to numerous fibroblasts (single arrows) within a fibroblastic focus (FF), in the epithelium surrounding a misshapen alveolus (Alv), and in endothelial cells (double arrows) near the FF. (C) Immunostaining for SP-C confirmed the alveolar type II cells within distorted, thickened alveolar regions (Alv). (D) Alpha-smooth muscle actin identified myofibroblasts (single arrows) in FF adjacent to an alveolus (Alv) and endothelial cells of small vessels having undergone endothelial–mesenchymal transition (double arrows). All sections were counterstained with methylene blue. Scale, 100 μm.

production, which was reduced by SB431542. Silencing Wnt7B greatly increased PAI-1 over shScramble controls, with or without Wnt7B overexpression (Fig. 8A). Normalized Vimentin levels did not change (data not shown). Similarly treated silenced hLF cells, which had not been transduced for overexpression, exhibited expression patterns for these proteins nearly identical to those of cells transduced with CMV-GFP (data not shown). Gene expression analysis confirmed the stimulatory influence of Wnt7B overexpression on *wnt5A* in hLFs, its decrease due to shWnt7B silencing, and its decrease with SB431542 (Fig. 8C).

In IPFF cells, cultured and transduced identically to hLFs as above, successful adenoviral transduction for forced expression of Wnt7B only modestly increased

Wnt5A protein expression (Fig. 9A, 9B). In all the CMV-GFP and the Wnt7B-shScramble-transduced cells, the normalized levels of Wnt5A were significantly reduced by SB431542 but, in CMV-Wnt7B + shWnt7B-silenced cells, SB431542 had a much less—although still significant—reducing effect (Fig. 9B). Wnt7B overexpression in control-silenced cells strongly increased α-SMA, which was reversed in shWnt7B-silenced cells; SB431542 had no effect (Fig. 9A). Control shScramble-silenced IPFF cells expressed PAI-1 strongly, which appeared resistant to downregulation by CMV-Wnt7B but was sensitive to SB431542. The strong downregulation of PAI-1 in shWnt7B-silenced cells when Wnt7B was overexpressed was reversed by SB431542. Normalized to the Vinculin loading control, Vimentin showed no changes
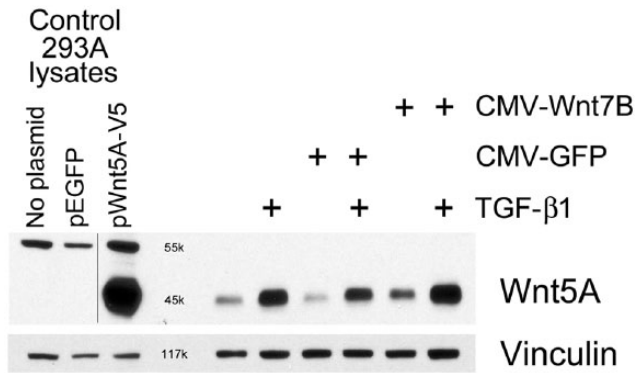
Figure 4. Western blot analysis of isolated normal human lung fibroblasts, untreated or transduced with CMV-GFP or CMV-Wnt7B adenovirus for 30 hr, then treated with or without 5 ng/ml TGF-β1 for 24 hr. Wnt7B overexpression (CMV-Wnt7B) and TGF-β1, separately, increased Wnt5A protein. This increase was enhanced by the combination of Wnt7B overexpression and TGF-β1. The positive staining reaction and appropriate molecular weight (~45 kDa) of the rhWnt5A-V5 band generated in pWnt5A-V5-transfected 293A cells and its absence in the pEGFP-transfected cells confirms the specificity of the CST 2530 anti-Wnt5A/B antibody. Vinculin was used as a loading control.
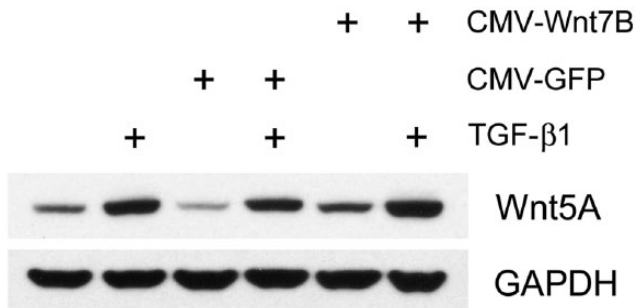

Figure 5. Western blot analysis of isolated normal human airway smooth muscle (hASMC) cells, untreated or transduced with CMV-GFP or CMV-Wnt7B adenovirus for 30 hr, then treated with or without 10 ng/ml TGF-β1 for 36 hr. Wnt7B overexpression (CMV-Wnt7B) and TGF-β1 treatment separately increased Wnt5A protein. This increase was enhanced further by CMV-Wnt7B and TGF-β1 together. GAPDH was used as a loading control.

Figure 6. Western blot analysis of day 5-isolated normal human alveolar type 2 (hAT2) cells, untreated or transduced with CMV-LacZ or CMV-Wnt7B adenovirus (20 MOI) for 30 hr, then treated with or without 10 ng/ml TGF-β1 for 24 hr. TGF-β1 alone had no effect on Wnt5A expression but, when added to CMV-LacZ-transduced cells, Wnt5A expression increased significantly. Successful Wnt7B overexpression did not significantly increase Wnt5A expression, and did not add to the TGF-β1-stimulated increase. Transfected 293A rhWnt5A-V5-positive and -negative lysates are as in Figure 4. Tubulin was used as a loading control. The chart illustrates the results of band density quantitation, with standard deviation error bars shown. *$p<0.05$, **$p<0.01$.

moderating effects in CMV-Wnt7B cells of combined shWnt7B silencing and SB431542 (Fig. 9C).

Discussion

In normal human lungs, relatively light immunohistochemical reactivity for Wnt5A was principally confined to airway epithelial cells, smooth muscle of airways and vessels, and a small subpopulation of interstitial fibroblasts, and more rarely was seen in some endothelial cells. The positive staining in smooth muscle cells and fibroblasts was confirmed by Wnt5A protein expression in isolated normal adult lung fibroblasts and airway smooth muscle cells. Wnt5A was not observed histochemically in normal alveolar epithelial cells (Fig. 1A, 1B), but it was detected by western blot in isolated day 5 primary hAT2 cells cultured on collagen matrix (Fig. 6). Recent data indicate that inhibition of Wnt5A expression abrogates the differentiation of isolated rat AT2 cells into AT1 cells, demonstrating its

due to treatment (data not shown). Similarly treated and silenced IPFF cells, which had not been transduced for overexpression, exhibited expression patterns that were nearly identical to those of CMV-GFP-transduced IPFF cells (data not shown). Gene expression analysis confirmed the minimal effect of forced Wnt7B overexpression on *wnt5A* in IPFFs; its decrease by SB431542 treatment and shWnt7B silencing, and by their combination in control overexpression and silenced cells; and the
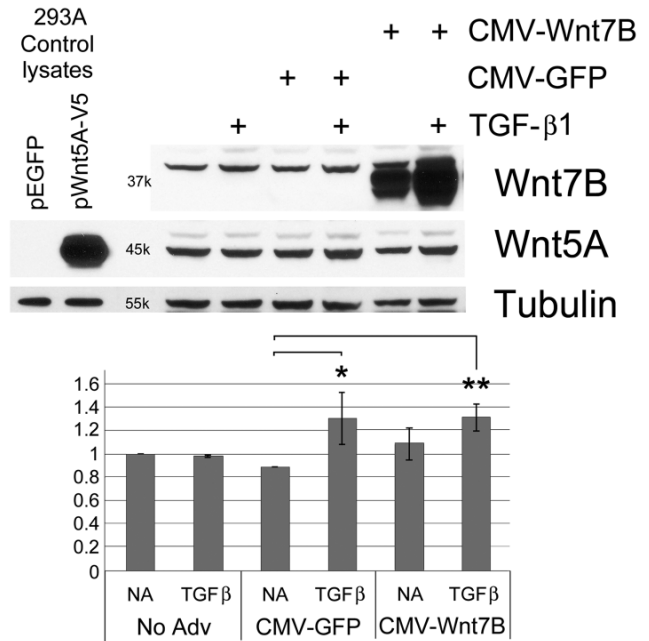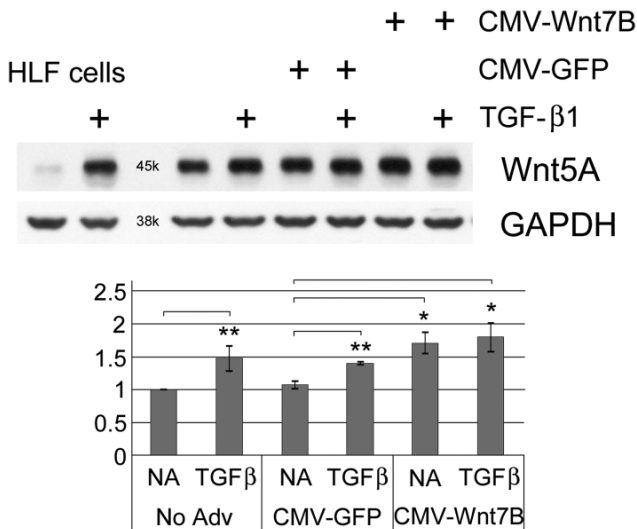
Figure 7. Western blot analysis of isolated fibroblasts/myofibroblasts (IPFFs) from a patient with idiopathic pulmonary fibrosis, untreated or transduced with adenoviruses for control (CMV-GFP) or Wnt7B overexpression (CMV-Wnt7B) for 30 hr, then treated with or without 5 ng/ml TGF-β1 for 24 hr. TGF-β1 treatment alone or with CMV-GFP had a significant effect on Wnt5A protein (**$p<0.01$). Although TGF-β1 and Wnt7B each significantly upregulated Wnt5A over untreated "No Adv" and "CVM-GFP" levels (*$p<0.05$), Wnt7B overexpression was statistically ineffective at increasing Wnt5A over levels induced by TGF-β1 alone. Untreated and TGF-β1-treated hLF cells are shown to compare the basal and stimulated levels of Wnt5A to those of IPFFs. GAPDH was used as a loading control. The chart illustrates the results of band density quantitation, with standard deviation error bars shown (*n*=3). Vinculin was used as loading control for chart and statistics.

contributions to alveolar maintenance in the normal lung (Ghosh et al. 2013). Interestingly, Wnt5A-related signaling is reported to contribute to the differentiation of mesenchymal stem cells into AT2 cells (Liu et al. 2014). Wnt5A gene expression has been shown to be high in isolated normal vascular smooth muscle cells and associated with ECM production (Zhu et al. 2013). It has also been demonstrated to be an important proliferation and survival factor for endothelial cells (Masckauchán et al. 2006) as well as a regulator of neovascularization (Murdoch et al. 2014). And in normal fibroblasts, Wnt5A promotes adhesion on collagen substrata (Kawasaki et al. 2007). Clearly a role for Wnt5A in lung homeostasis is beginning to emerge, giving context to the histochemical localization seen here in normal lung.

In lungs from patients with IPF, the wide distribution of Wnt5A in myofibroblasts of FF and throughout the interstitium was impressive but largely confirmatory, as its high level of gene and protein expression was previously established (Vuga et al. 2009). It was further demonstrated that
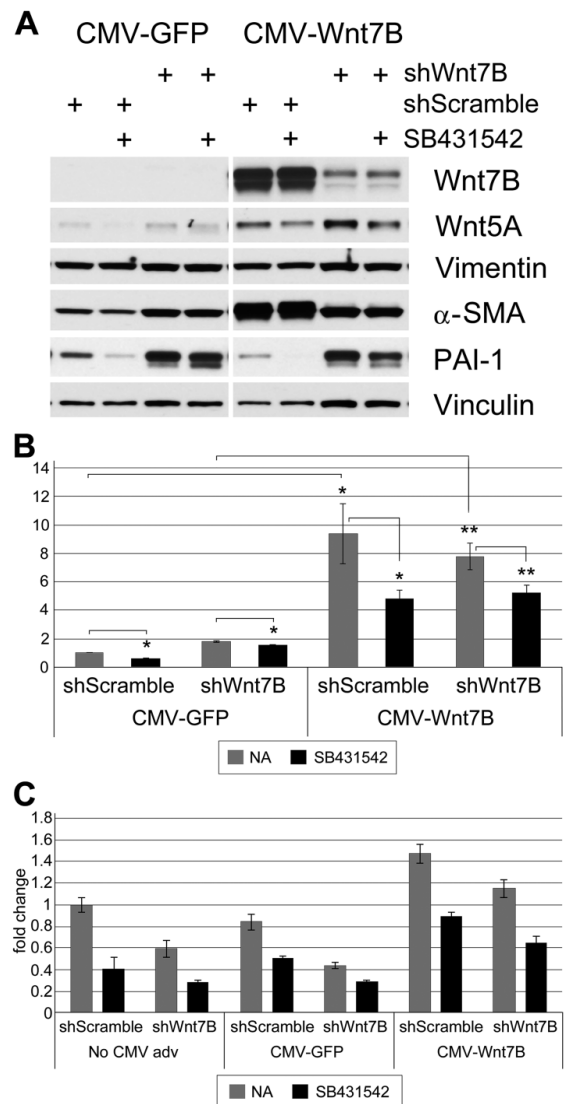

Figure 8. Wnt5A expression in shWnt7B-silenced normal human lung fibroblasts (hLFs) or overexpressing Wnt7B when TGF-β1 signaling is inhibited. Normal hLFs were adenovirally transduced to silence Wnt7B (shWnt7B) or with silencing Control (shScramble) before adenoviral transduction with CMV-Wnt7B or with CMV-GFP adenovirus. Some cells were subsequently treated with vehicle or 10 μM SB431542 (TGF-β1 Receptor kinase inhibitor) for an additional 24 hr. (A) Western blot. Silenced hLF cells not transduced for overexpression exhibited responses very similar to those of silenced CMV-GFP-transduced cells (data not shown). Each band is from the same exposure of the same representative western blot. Vinculin was used as loading control. (B) Quantitation of Wnt5A protein expression, normalized to Vinculin. Wnt7B overexpression strongly upregulates Wnt5A, and SB431542 counteracts this upregulation. *$p<0.05$, **$p<0.01$. (C) TaqMan gene expression analysis of *wnt5A* gene expression, normalized to *gapdh*, is shown as fold-changes relative to "No CMV adv, shScramble, NA". CMV-Wnt7B in hLF cells increases *wnt5A* over baseline expression, silencing Wnt7B reverses this, and in "CMV-Wnt7B + shWnt7B + SB" cells, inhibition of TGF-β1 signaling further reduces *wnt5A* gene expression.
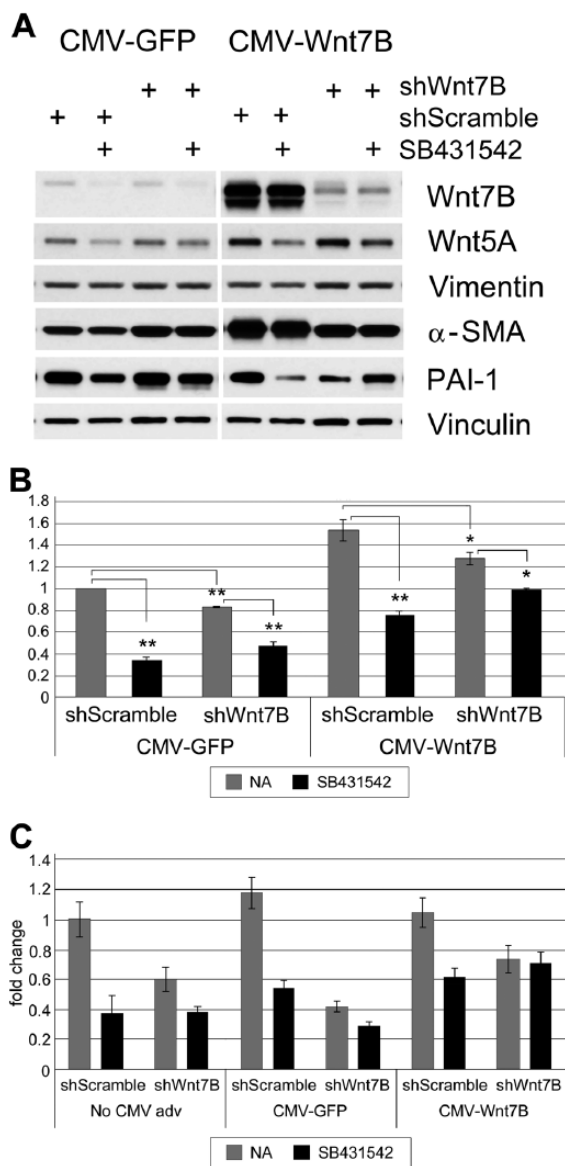
Figure 9. Wnt5A expression in shWnt7B-silenced IPF fibroblasts/myofibroblasts (IPFFs) or overexpressing Wnt7B when TGF-β1 signaling is inhibited. IPFF cells were transduced and treated as in Figure 8. (A) Western blot. Silenced IPFF cells not transduced for overexpression exhibited responses very similar to those of silenced CMV-GFP-transduced cells (data not shown). Vinculin was used as loading control. Each band is from the same exposure of the same representative western blot. (B) Quantitation of Wnt5A, normalized to Vinculin. Wnt7B overexpression modestly upregulates Wnt5A, and shWnt7B significantly counteracts this upregulation. SB431542 is effective in knocking down Wnt5A expression in shScramble cells but is less effective in "CMV-Wnt7B + shWnt7B" cells. *$p<0.05$, **$p<0.01$. (C) TaqMan gene expression analysis of *wnt5A* gene expression, normalized to *gapdh*, is shown as fold-changes relative to "No CMV adv, shScramble, NA". In these IPFF cells, Wnt7B overexpression does not increase *wnt5A* over baseline expression, and in "CMV-Wnt7B + shWnt7B" cells, the TGF-β1 signaling inhibitor, SB431542, has no effect.

Wnt5A in UIP fibroblasts promotes proliferation and resistance to H_2O_2-induced apoptosis (Vuga et al. 2009). It is perhaps relevant that non-canonical Wnt5A signaling, an important characteristic of IPF (Willis et al. 2006), regulates epithelial-mesenchymal transition (EMT) in metastatic lung cancer (Gujral et al. 2014). It would not be surprising, therefore, that Wnt5A expression in IPF epithelial cells would play a contributory role in EMT processes that might add to the myofibroblast burden in IPF.

It is well established that TGF-β is produced by epithelial cells in patients with IPF (Khalil et al. 1991) and is a key modulator of ECM production in fibrogenic processes (Lasky and Brody 2000). These findings helped develop the functional linkage between epithelial cells as effectors in the fibrogenic process and fibroblasts as key responders in ECM production. Recent studies on hASMC cells from asthmatics demonstrated that Wnt5A was upregulated and could be markedly induced in response to TGF-β (Kumawat et al. 2013). Importantly, they also showed that inhibition of Wnt5A attenuated ECM production. This raised the issues of whether a TGF-β1–Wnt5A linkage exists in the IPF lung and, if so, whether other signaling factors localized within the fibrotic regions could be involved as well. By virtue of its epithelial localization and unique distribution within FF, Wnt7B became an intriguing candidate (Meuten et al. 2012). Indeed, the forced expression of Wnt7B in normal hLFs resulted in increases in Wnt5A protein (Figs. 4, 8A, 8B) and gene (Fig. 8C) expression. In combination with free TGF-β1, Wnt7B overexpression elevated Wnt5A levels even further (Fig. 4). This presumed co-regulation of Wnt5A by TGF-β1 and Wnt7B in normal fibroblasts is tempered by shRNA inhibition of Wnt7B overexpression, which reduced Wnt5A protein somewhat while, even in the absence of added TGF-β1, TGF-β1 receptor kinase inhibition reduced Wnt5A significantly (Figs. 8A, 8B). This would argue that at least part of Wnt7B's action on Wnt5A may be due to crosstalk with constitutive levels of endogenous TGF-β1. Perhaps relatedly, it is notable that the IPFF had a similar profile of Wnt5A gene and protein expression (Figs. 8A, 8C vs Figs. 9A, 9C), but the response of Wnt7B-silenced cells to Wnt7B overexpression with concomitant TGF-β1 signaling inhibition was somewhat muted. These shifts in responsiveness could perhaps be due to differences in receptor expression between normal fibroblasts, exposed to multiple stimuli, and mature (IPFF) myofibroblasts with a higher proportion of their energy invested in higher basal Wnt5A levels and matrix-related signaling.

Previous studies have shown synergistic interactions between Wnt proteins and TGF-β signaling pathways. Zhou and colleagues (2004) showed that TGF-β upregulates multiple Wnts and increases the nuclear accumulation and stability of β-catenin in human mesenchymal stem cells during their differentiation. Baarsma et al. (2011) have demonstrated that TGF-β1 induces Wnt5B expression and activates β-catenin in

fibroblasts from normal and COPD (emphysema) lungs. They further showed that inhibition of β-catenin reduced TGF-β1-induced α-SMA expression but had no effect on TGF-β1-induced PAI-1. We show here that Wnt7B overexpression in the absence of added TGF-β1 increased α-SMA, an effect attenuated by shWnt7B but not by SB431542, in agreement with its probable β-catenin-mediated signaling. Further, the overexpression of Wnt7B had little effect on PAI-1 whereas silencing Wnt7B enhanced PAI-1 and afforded some resistance to the effects of SB431542 inhibition of TGF-β1 signaling, which reduced PAI-1. The variable responses of hLFs and IPFFs may reflect the Wnt and TGF-β1 pathway crosstalk that directs concentration-dependent pathway activation of target genes (Baarsma et al. 2011), and suggest the possibility of an additional unknown mediator, perhaps Wnt5A itself. The prospect of the involvement of other Wnts is under investigation.

The widespread expression of Wnt5A in smooth muscle in IPF lungs was notable and parallels the strong expression of Wnt7B (Meuten et al. 2012) and FGF9 (Coffey et al. 2013). The presence of Wnt7B in smooth muscle could easily explain the enhanced expression of Wnt5A in smooth muscle cells of IPF lungs, which is supported by results of Wnt7B forced expression in isolated hASMCs (Fig. 5). The study of Kumawat et al. (2013) has serious implications for the potential role for smooth muscle in IPF, relating to ECM production. Ohta et al. (1995) suggested this in an earlier study, which demonstrated the wide distribution of smooth muscle in IPF lungs, in both tightly packed and disorganized bundles as well as isolated individual fibers, some of which stained positively for procollagen I. More work will be necessary to fully establish a role for smooth muscle and ECM expansion in IPF, but the localization of Wnt7B, and now Wnt5A, presents intriguing support of this notion.

Lastly, the increased reactivity of vascular endothelium in IPF (Fig. 3B) is of interest, especially in light of evidence for endothelial-mesenchymal transition (EnMT) in vascular remodeling (Coll-Bonfill et al. 2015) and its important contributing influence in IPF (Barratt and Millar 2014). Data have previously shown that Wnt7B is found in small vascular structures near FF and throughout the interstitium of IPF lungs (Meuten et al. 2012), and now Wnt5A is demonstrated in these same structures along with α-SMA. We further demonstrate here that forced expression of Wnt7B increases both Wnt5A and α-SMA in hLFs and IPFFs. Evidence indicates that Wnt5A is elevated in lung cancer cell lines and drives both EMT and migration via the Frizzled2 receptor (Gujral et al. 2014). The linkage between Wnt7B–Wnt5A expression in much of the vasculature of IPF lungs as a possible indicator of EnMT offers yet another potential mechanism for advancing the pathological growth and distortion of the pulmonary ECM.

These studies suggest that each lung cell type may respond differently in health and disease to the varying concentrations of Wnt7B and TGF-β1 in their microenvironments and may also be affected by their neighboring cells' changes in expression of these and other factors with progression of the disease. Indeed, we saw a significant TGF-β1-stimulated increase in Wnt5A expression in hAT2 cells only when they were also transduced with adenoviruses, and an IPF-virus connection has long been suspected. Perhaps infection with certain viruses triggers the initial steps in the development of IPF in certain genetic backgrounds. In the normal lung fibroblasts and airway smooth muscle cells studied here, Wnt7B and TGF-β1 added to each other's stimulation of Wnt5A expression. But in IPFFs, an already high level of Wnt5A expression resisted both further stimulation (Fig. 7) and its reduction by Wnt7B silencing and TGF-β1 signaling inhibition (Fig. 9). One might envision that the increased expression of Wnt5A by lung fibroblasts or smooth muscle cells, triggered perhaps by aberrant or over-enthusiastic growth factor production by macrophages or lung epithelium in the wake of injury or infection, could result in the production of excess matrices and molecules that mute or even reverse homeostatic efforts of the lung and cause it to fail to resolve. The high level of expression of both PAI-1 and α-SMA in IPF fibroblasts and their continued expression in the presence of an inhibitor of TGF-β1 signaling suggests that, although TGF-β1 may help trigger the initial proliferation of matrix-producing, mobile fibroblasts, at some point it may become dispensable.

Author Contributions

DRN designed, performed, and analyzed experiments, isolated and cultured primary cells, prepared adenoviral constructs, and edited the paper; WSS performed IHC-P; KH, AZ, KMT, and EC performed and analyzed experiments; PLS designed experiments, performed IHC-P and microscopy, and drafted and edited the paper.

Competing Interests

The authors declared no potential conflicts of interest with respect to the research, authorship, and/or publication of this article.

References

Apparao KB, Newman DR, Zhang H, Khosla J, Randell SH, Sannes PL (2010). Temporal changes in expression of FoxA1 and Wnt7A in isolated adult human alveolar epithelial cells enhanced by heparin. Anat Rec. (Hoboken) 293:938-946.

Baarsma HA, Spanjer AIR, Haitsma G, Engelbertink LHJM, Meurs H, Jonker MR, Timens W, Postma DS, Kerstjens HAM, Gosens R (2011). Activation of WNT/β-catenin signaling in pulmonary fibroblasts by TGF-β$_1$ is increased in chronic obstructive pulmonary disease. PLoS ONE 6: e25450.

Barratt S, Millar A (2014). Vascular remodelling in the pathogenesis of idiopathic pulmonary fibrosis. QJM 107:515-519.

Boucherat O, Franco-Montoya ML, Thibault C, Incitti R, Chailley-Heu B, Delacourt C, Bourbon JR (2007). Gene expression profiling in lung fibroblasts reveals new players in alveolarization. Physiol Genomics 32:128-141.

Broekelmann TJ, Limper AH, Colby TV, McDonald JA (1991). Transforming growth factor beta 1 is present at sites of extracellular matrix gene expression in human pulmonary fibrosis. Proc Natl Acad Sci U S A 88:6642-6646.

Chilosi M, Poletti V, Zamo A, Lestani M, Montagna L, Piccoli P, Pedron S, Bertaso M, Scarpa A, Murer B, Cancellieri A, Maestro R, Semenzato G, Doglioni C (2003). Aberrant Wnt/beta-catenin pathway activation in idiopathic pulmonary fibrosis. Am J Pathol 162:1495-1502.

Coffey E, Newman DR, Sannes PL (2013). Expression of fibroblast growth factor 9 in normal human lung and idiopathic pulmonary fibrosis. J Histochem Cytochem 61:671-679.

Coll-Bonfill N, Musri MM, Ivo V, Barberà JA, Tura-Ceide O (2015). Transdifferentiation of endothelial cells to smooth muscle cells play an important role in vascular remodelling. Am J Stem Cells 4:13-21.

Cool CD, Groshong SD, Rai PR, Henson PM, Stewart JS, Brown KK (2006). Fibroblast foci are not discrete sites of lung injury or repair: the fibroblast reticulum. Am J Respir Crit Care Med 174:654-658.

Cornett B, Snowball J, Varisco BM, Lang R, Whitsett J, Sinner D (2013). Wntless is required for peripheral lung differentiation and pulmonary vascular development. Dev Biol 379:38-52.

Dobbs LG, Gonzales R, Williams MC (1986). An improved method for isolating type II cells in high yield and purity. Am Rev Respir Dis 134:141-145.

Fernandez IE, Eickelberg O (2012). The impact of TGF-beta on lung fibrosis: from targeting to biomarkers. Proc Am Thorac Soc 9:111-116.

Ghosh MC, Gorantla V, Makena PS, Luellen C, Sinclair SE, Schwingshackl A, Waters CM (2013). Insulin-like growth factor-I stimulates differentiation of ATII cells to ATI-like cells through activation of Wnt5a. Am J Physiol Lung Cell Mol Physiol 305:L222-L228.

Green FH (2002). Overview of pulmonary fibrosis. Chest 122:334S-339S.

Gujral TS, Chan M, Peshkin L, Sorger PK, Kirschner MW, MacBeath G (2014). A noncanonical Frizzled2 pathway regulates epithelial-mesenchymal transition and metastasis. Cell 159:844-856.

Kapanci Y, Desmouliere A, Pache JC, Redard M, Gabbiani G (1995). Cytoskeletal protein modulation in pulmonary alveolar myofibroblasts during idiopathic pulmonary fibrosis. Possible role of transforming growth factor beta and tumor necrosis factor alpha. Am J Respir Crit Care Med 152:2163-2169.

Katzenstein AL, Myers JL (1998). Idiopathic pulmonary fibrosis: clinical relevance of pathologic classification. Am J Respir Crit Care Med 157:1301-1315.

Katzenstein AL, Zisman DA, Litzky LA, Nguyen BT, Kotloff RM (2002). Usual interstitial pneumonia: histologic study of biopsy and explant specimens. Am J Surg Pathol 26:1567-1577.

Kawasaki A, Torii K, Yamashita Y, Nishizawa K, Kanekura K, Katada M, Ito M, Nishimoto I, Terashita K, Aiso S, Matsuoka M (2007). Wnt5a promotes adhesion of human dermal fibroblasts by triggering a phosphatidylinositol-3 kinase/Akt signal. Cell Signal 19:2498-2506.

Khalil N, O'Connor RN, Unruh HW, Warren PW, Flanders KC, Kemp A, Bereznay OH, Greenberg AH (1991). Increased production and immunohistological localization of transforming growth factor-beta in idiopathic pulmonary fibrosis. Am J Respir Cell Mol Biol 5:155-162.

Konigshoff M, Balsara N, Pfaff EM, Kramer M, Chrobak I, Seeger W, Eickelberg O (2008). Functional Wnt signaling is increased in idiopathic pulmonary fibrosis. PLoS One 3:e2142.

Kumawat K, Menzen MH, Bos IS, Baarsma HA, Borger P, Roth M, Tamm M, Halayko AJ, Simoons M, Prins A, Postma DS, Schmidt M, Gosens R (2013). Noncanonical WNT-5A signaling regulates TGF-β-induced extracellular matrix production by airway smooth muscle cells. FASEB J 27:1631-1643.

Lasky JA, Brody AR (2000). Interstitial fibrosis and growth factors. Environ Health Perspect 108(Suppl 4):751-762.

Levänen B, Wheelock AM, Eklund A, Grunewald J, Nord M (2011). Increased pulmonary Wnt (wingless/integrated)-signaling in patients with sarcoidosis. Respir Med 105:282-291.

Li C, Xiao J, Hormi K, Borok Z, Minoo P (2002). Wnt5a participates in distal lung morphogenesis. Dev Biol 248:68-81.

Li C, Hu L, Xiao J, Chen H, Li JT, Bellusci S, Delanghe S, Minoo P (2005). Wnt5a regulates Shh and Fgf10 signaling during lung development. Dev Biol 287:86-97.

Liu A, Chen S, Cai S, Dong L, Liu L, Yang Y, Guo F, Lu X, He H, Chen Q, Hu S, Qiu H (2014). Wnt5a through noncanonical Wnt/JNK or Wnt/PKC signaling contributes to the differentiation of mesenchymal stem cells into type II alveolar epithelial cells in vitro. PLoS One 9:e90229.

Loscertales M, Mikels AJ, Hu JK, Donahoe PK, Roberts DJ (2008). Chick pulmonary Wnt5a directs airway and vascular tubulogenesis. Development 135:1365-1376.

MacDonald BT, Hien A, Zhang X, Iranloye O, Virshup DM, Waterman ML, He X (2014). Disulfide bond requirements for active Wnt ligands. J Biol Chem 289:18122-18136.

Masckauchán TN, Agalliu D, Vorontchikhina M, Ahn A, Parmalee NL, Li CM, Khoo A, Tycko B, Brown AM, Kitajewski J

(2006). Wnt5a signaling induces proliferation and survival of endothelial cells in vitro and expression of MMP-1 and Tie-2. Mol Biol Cell 17:5163-5172.

Meuten T, Hickey A, Franklin K, Grossi B, Tobias J, Newman DR, Jennings SH, Correa M, Sannes PL (2012). WNT7B in fibroblastic foci of idiopathic pulmonary fibrosis. Respir Res 13:62.

Morrisey EE (2003). Wnt signaling and pulmonary fibrosis. Am J Pathol 162:1393-1397.

Murdoch CE, Bachschmid MM, Matsui R (2014). Regulation of neovascularization by S-glutathionylation via the Wnt5a/sFlt-1 pathway. Biochem Soc Trans 42:1665-1670.

Ohta K, Mortenson RL, Clark RA, Hirose N, King TE, Jr (1995). Immunohistochemical identification and characterization of smooth muscle-like cells in idiopathic pulmonary fibrosis. Am J Respir Crit Care Med 152:1659-1665.

Rajagopal J, Carroll TJ, Guseh JS, Bores SA, Blank LJ, Anderson WJ, Yu J, Zhou Q, McMahon AP, Melton DA (2008). Wnt7b stimulates embryonic lung growth by coordinately increasing the replication of epithelium and mesenchyme. Development 135:1625-1634.

Rashid ST, Humphries JD, Byron A, Dhar A, Askari JA, Selley JN, Knight D, Goldin RD, Thursz M, Humphries MJ (2012). Proteomic analysis of extracellular matrix from the hepatic stellate cell line LX-2 identifies CYR61 and Wnt-5a as novel constituents of fibrotic liver. J Proteome Res 11:4052-4064.

Salazar KD, Lankford SM, Brody AR (2009). Mesenchymal stem cells produce Wnt isoforms and TGF-beta1 that mediate proliferation and procollagen expression by lung fibroblasts. Am J Physiol Lung Cell Mol Physiol 297:L1002-L1011.

Schwartz DA, Helmers RA, Galvin JR, Van Fossen DS, Frees KL, Dayton CS, Burmeister LF, Hunninghake GW (1994). Determinants of survival in idiopathic pulmonary fibrosis. Am J Respir Crit Care Med 149:450-454.

Scotton CJ, Chambers RC (2007). Molecular targets in pulmonary fibrosis: the myofibroblast in focus. Chest 132:1311-1321.

Villar J, Cabrera NE, Casula M, Valladares F, Flores C, López-Aguilar J, Blanch L, Zhang H, Kacmarek RM, Slutsky AS (2011). WNT/β-catenin signaling is modulated by mechanical ventilation in an experimental model of acute lung injury. Intensive Care Med 37:1201-1209.

Vuga LJ, Ben-Yehudah A, Kovkarova-Naumovski E, Oriss T, Gibson KF, Feghali-Bostwick C, Kaminski N (2009). WNT5A is a regulator of fibroblast proliferation and resistance to apoptosis. Am J Respir Cell Mol Biol 41:583-589.

Willis BC, duBois RM, Borok Z (2006). Epithelial origin of myofibroblasts during fibrosis in the lung. Proc Am Thorac Soc 3:377-382.

Zhang H, Newman DR, Sannes PL (2012). HSULF-1 inhibits ERK and AKT signaling and decreases cell viability in vitro in human lung epithelial cells. Respir Res 13:69.

Zhou S, Eid K, Glowacki J (2004). Cooperation between TGF-beta and Wnt pathways during chondrocyte and adipocyte differentiation of human marrow stromal cells. J Bone Miner Res 19:463-470.

Zhu TX, Lan B, Meng LY, Yang YL, Li RX, Li EM, Zheng SY, Xu LY (2013). ECM-related gene expression profile in vascular smooth muscle cells from human saphenous vein and internal thoracic artery. J Cardiothorac Surg 18:155.